



# Investigating the Efficacy of Triple Artemisinin-Based Combination Therapies for Treating *Plasmodium falciparum* Malaria Patients Using Mathematical Modeling

Saber Dini,<sup>a</sup>  Sophie Zaloumis,<sup>a</sup> Pengxing Cao,<sup>b</sup> Ric N. Price,<sup>c,d</sup> Freya J. I. Fowkes,<sup>a,e,f</sup> Rob W. van der Pluijm,<sup>d,g</sup> James M. McCaw,<sup>a,b,h,i</sup> Julie A. Simpson<sup>a</sup>

<sup>a</sup>Centre for Epidemiology and Biostatistics, Melbourne School of Population and Global Health, University of Melbourne, Melbourne, Australia

<sup>b</sup>School of Mathematics and Statistics, University of Melbourne, Melbourne, Australia

<sup>c</sup>Global and Tropical Health Division, Menzies School of Health Research and Charles Darwin University, Casuarina, Australia

<sup>d</sup>Centre for Tropical Medicine and Global Health, Nuffield Department of Clinical Medicine, University of Oxford, Oxford, United Kingdom

<sup>e</sup>Burnet Institute, Disease Elimination Program, Public Health, Melbourne, Australia

<sup>f</sup>Department of Epidemiology and Preventative Medicine and Department of Infectious Diseases, Monash University, Melbourne, Australia

<sup>g</sup>Mahidol Oxford Tropical Medicine Research Unit, Bangkok, Thailand

<sup>h</sup>Peter Doherty Institute for Infection and Immunity, The Royal Melbourne Hospital and University of Melbourne, Melbourne, Australia

<sup>i</sup>Murdoch Children's Research Institute, The Royal Children's Hospital, Melbourne, Australia

**ABSTRACT** The first line treatment for uncomplicated falciparum malaria is artemisinin-based combination therapy (ACT), which consists of an artemisinin derivative coadministered with a longer-acting partner drug. However, the spread of *Plasmodium falciparum* resistant to both artemisinin and its partner drugs poses a major global threat to malaria control activities. Novel strategies are needed to retard and reverse the spread of these resistant parasites. One such strategy is triple artemisinin-based combination therapy (TACT). We developed a mechanistic within-host mathematical model to investigate the efficacy of a TACT (dihydroartemisinin-piperazine-mefloquine [DHA-PPQ-MQ]) for use in South-East Asia, where DHA and PPQ resistance are now increasingly prevalent. Comprehensive model simulations were used to explore the degree to which the underlying resistance influences the parasitological outcomes. The effect of MQ dosing on the efficacy of TACT was quantified at various degrees of DHA and PPQ resistance. To incorporate interactions between drugs, a novel model is presented for the combined effect of DHA-PPQ-MQ, which illustrates how the interactions can influence treatment efficacy. When combined with a standard regimen of DHA and PPQ, the administration of three 6.7-mg/kg doses of MQ was sufficient to achieve parasitological efficacy greater than that currently recommended by World Health Organization (WHO) guidelines. As a result, three 8.3-mg/kg doses of MQ, the current WHO-recommended dosing regimen for MQ, combined with DHA-PPQ, has the potential to produce high cure rates in regions where resistance to DHA-PPQ has emerged.

**KEYWORDS** antimalarial agents, artemisinin-based combination therapy, drug efficacy, drugs interactions, mathematical modeling

Over the last decade, significant gains have been made towards the control and elimination of malaria. Despite this progress, almost half a million people still die from malaria each year. Disturbingly, in 2016 there were five million more cases of

Received 24 May 2018 Returned for modification 1 July 2018 Accepted 7 August 2018

Accepted manuscript posted online 27 August 2018

**Citation** Dini S, Zaloumis S, Cao P, Price RN, Fowkes FJI, van der Pluijm RW, McCaw JM, Simpson JA. 2018. Investigating the efficacy of triple artemisinin-based combination therapies for treating *Plasmodium falciparum* malaria patients using mathematical modeling. *Antimicrob Agents Chemother* 62:e01068-18. <https://doi.org/10.1128/AAC.01068-18>.

**Copyright** © 2018 Dini et al. This is an open-access article distributed under the terms of the [Creative Commons Attribution 4.0 International license](https://creativecommons.org/licenses/by/4.0/).

Address correspondence to Julie A. Simpson, [julieas@unimelb.edu.au](mailto:julieas@unimelb.edu.au).

malaria than the previous year (according to the World Health Organization [WHO] in 2017 [1]), emphasizing the fragile nature of malaria control. Early diagnosis and treatment with highly effective antimalarial drug regimens remains central to all national malaria control activities. Artemisinin-based combination therapies (ACTs) are the first-line therapy in almost all countries where malaria is endemic due to the high efficacy, tolerability, and ability of ACTs to reduce ongoing transmission of the parasite. ACTs are comprised of two components: an artemisinin derivative and a partner drug. The artemisinin derivative has a high antimalarial potency, killing a large proportion of parasites; however, these compounds are rapidly eliminated, leaving a residual parasite population that, if left untreated, will likely recrudescence. A slowly eliminated partner drug is required to provide a sustained antimalarial activity that is capable of killing the remaining parasites (2).

ACTs have remained highly efficacious for almost 2 decades but are now under threat from the emergence of drug-resistant parasites (2, 3). In 2009, a high proportion of patients with markedly delayed parasite clearance were reported from the western region of Cambodia, and this was confirmed as being attributable to artemisinin resistance (3). These parasites have now spread across the Greater Mekong Region (4, 5). Delayed parasite clearance and higher gametocyte carriage, due to the artemisinin derivative resistance, drive the selection of resistance to the partner drug (6), and in South-East Asia this has resulted in declining efficacy of all the ACTs currently recommended by WHO (7). In some parts of the Greater Mekong Region, the spread of highly drug-resistant parasites poses a major threat to malaria control activities. The emergence of an untreatable *P. falciparum* will result in an inevitable rise in malaria incidence, epidemics, and associated morbidity and mortality.

The development of alternative strategies is crucial to ensuring the ongoing success of malaria control efforts. Triple Artemisinin-based Combination Therapy (TACT) is a novel strategy by which a new partner drug is added to an established ACT. TACT has the potential to decrease the chance of emergence of a *de novo* resistance, as well as rescuing a regimen in which one of the ACT components is already failing. Two antimalarial clinical trials are under way to determine the efficacy of TACT for uncomplicated falciparum malaria: Artemether-Lumefantrine plus Amodiaquine (AL-AQ) and Dihydroartemisinin-Piperaquine plus Mefloquine (DHA-PPQ-MQ). These are being compared to the standard ACTs (AL and DHA-PPQ) alone (see trial NCT02453308 at [clinicaltrials.gov](http://clinicaltrials.gov)).

In the present study, we developed a within-host mathematical model (8) to explore the efficacy of TACTs, with a particular focus on DHA-PPQ-MQ, since DHA-PPQ is widely administered in South-East Asia and is currently associated with very high failure rates in some regions (9–11). The model accommodates a high level of biological details, such as drug-drug interaction (12, 13), the stage specificity of parasite killing (14–17), and between-patient and between-isolate variability (17). We used the model to simulate different levels of resistance and quantify the degree to which this compromises the efficacy of TACT. The optimal MQ dosing regimen was determined for various degrees of resistance to DHA-PPQ.

## RESULTS

Figure 1 shows examples of drug concentration profiles for DHA, PPQ, and MQ and the corresponding parasitemia profiles obtained from model simulations. WHO-recommended dosing regimens were used in the simulations, i.e., 18.0 mg/kg/day of PPQ, 4.0 mg/kg/day of DHA, and 8.3 mg/kg/day of MQ for 3 days. The median concentrations of the drugs (lines), along with the between-subject variabilities (the shaded regions show the area between the 2.5 and 97.5% percentiles), are presented in Fig. 1a, and the parasitemia of 100 randomly selected patients in Fig. 1b. Figure 1c presents the Kaplan-Meier estimation of the probability of cure, along with the 95% confidence intervals illustrated by the shaded region.

Parasite resistance to antimalarial drugs can manifest in a couple of different ways that affect the killing profile of a drug (see the concentration-effect curves in Fig. 2).

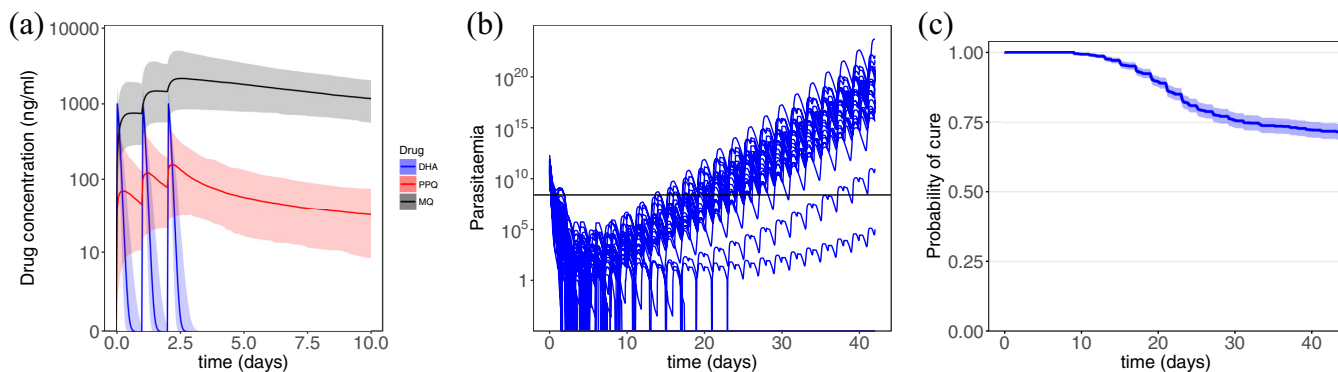


**FIG 1** Model simulation. (a) PK model results. The concentrations of DHA (blue), PPQ (red), and MQ (black) are depicted. The shaded regions show the area between the 2.5th and 97.5th percentiles of the results generated for 1,000 patients. (b) PD model results for 100 randomly selected patients. The horizontal line shows the microscopic level of detection of parasites. (c) Kaplan-Meier estimation of the probability of survival over 42 days of follow-up.

These include (i) increasing the 50% effective concentration ( $EC_{50}$ ; the red curve), (ii) reducing the size of the killing window in the intraerythrocytic parasite life cycle,  $W$ , and (iii) decreasing the sigmoidicity,  $\gamma$ , and/or maximum killing effect,  $E_{max}$  (the blue curve). The degree of resistance was modeled initially by varying the  $EC_{50}$  values of PPQ, in scenarios where the parasites are sensitive or resistant to DHA. The influence of other manifestations of resistance on TACT efficacy are outlined in the supplemental material.

The level of resistance and the resultant risk of treatment failure varies with geographical region. Table 1 demonstrates a large variation in DHA-PPQ efficacy in different regions across South-East Asia (18). The risk of failures in Aoral and Chi Kraeng in Cambodia are 51.9 and 62.5% treatment failures, respectively, whereas in Siem Pang it is only 8.3%. Similar large variations in the probability of treatment failure are observed in Vietnam. According to the WHO treatment guidelines, when the risk of failure exceeds 10%, a treatment is considered suboptimal, and steps should be taken to change the policy to a more efficacious antimalarial regimen.

**Artemisinin sensitivity.** In the first investigated scenario, the parasites were assumed to be sensitive to DHA (the sampling interval of  $EC_{50,D}$  was limited to (1,10] ng/ml), and the resistance level to PPQ was varied. Figure 3a shows how the probability of cure at day 42 of follow-up varies with  $EC_{50}$  of PPQ over the deciles of (11,94] ng/ml. The top labels in this figure show the geographical regions in South-East Asia (Table 1)

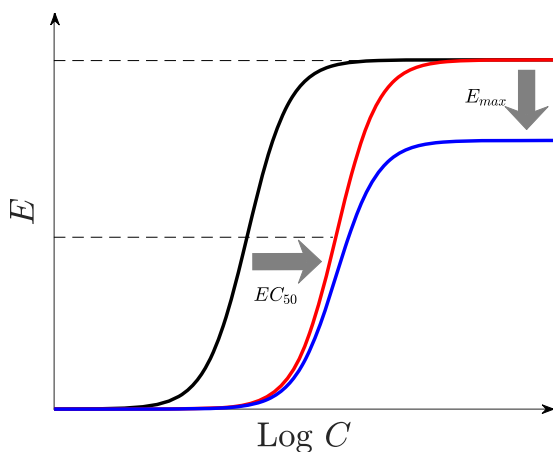


**FIG 2** Resistance manifestations. The graph shows the resistance of parasites to drugs, modeled by relevant alterations of the parameters of the model. A concentration-effect profile of susceptible parasites (black) can be right-shifted, i.e., the  $EC_{50}$  increases (red) and/or the maximum killing effect,  $E_{max}$ , decreases (blue).

**TABLE 1** Kaplan-Meier estimation of the probabilities of cure on day 42 of follow-up in some regions in South-East Asia where DHA-PPQ is the first-line treatment for malaria<sup>a</sup>

| Parameter           | Geographical region |            |            |          |            |
|---------------------|---------------------|------------|------------|----------|------------|
|                     | Siem Pang           | Binh Phuoc | Bu Gia Map | Aoral    | Chi Kraeng |
| Probability of cure | 0.92                | 0.74       | 0.67       | 0.48     | 0.38       |
| No. of patients     | 60                  | 40         | 40         | 53       | 40         |
| Yr                  | 2015                | 2015       | 2015       | 2015     | 2014       |
| Country             | Cambodia            | Viet Nam   | Viet Nam   | Cambodia | Cambodia   |

<sup>a</sup>World Health Organization (18).

that have observed DHA-PPQ day 42 cure rates equal to the corresponding simulated values (18).

The probability of cure declines as the EC<sub>50</sub> of PPQ increases. Without MQ, the probability of cure with DHA-PPQ is below 90%, over EC<sub>50,P</sub> ∈ (45,94], which includes Binh Phuoc and Bu Gia Map. This scenario was unable to produce the probabilities of cure observed in all of the geographical regions, shown in Table 1.

The addition of a 10-mg/kg total dose of MQ (3.3 mg/kg/day for 3 days) significantly raised the probability of cure. The improvement in efficacy with this regimen of MQ was insufficient to ensure successful treatment in Bu Gia Map. In this region, 15-mg/kg dose of MQ (5 mg/kg/day for 3 days) was required. When the parasites are sensitive to DHA but resistant to PPQ, MQ at 15 mg/kg was sufficient to achieve cure in all locations. Administration of 20 mg/kg (6.7 mg/kg/day for 3 days) or 25 mg/kg (8.3 mg/kg/day for 3 days) did not provide significant benefit over the 15-mg/kg regimen, although this might be used to guarantee the success of the TACT.

**Artemisinin resistance.** Concurrent resistance to DHA and PPQ is now documented in Cambodia and Vietnam (9, 10). To simulate a high level of DHA resistance, we set EC<sub>50,D</sub> ∈ (50,100] ng/ml and varied the intensity of resistance to PPQ, EC<sub>50,P</sub> ∈ (11,94] ng/ml. Using the same dosing regimens as those in Fig. 3a, resistance to DHA leads to a significant decline in the efficacy of DHA-PPQ, as shown in Fig. 3b. When combined with a 10-mg/kg dose of MQ, the efficacy of the TACT was improved significantly, but except for Siem Pang it was clearly not sufficient.

Administration of a 15-mg/kg dose of MQ provided sufficient efficacy in Binh Phuoc and Bu Gia Map but was still insufficient for Aoral and Chi Kraeng. At least a 20-mg/kg

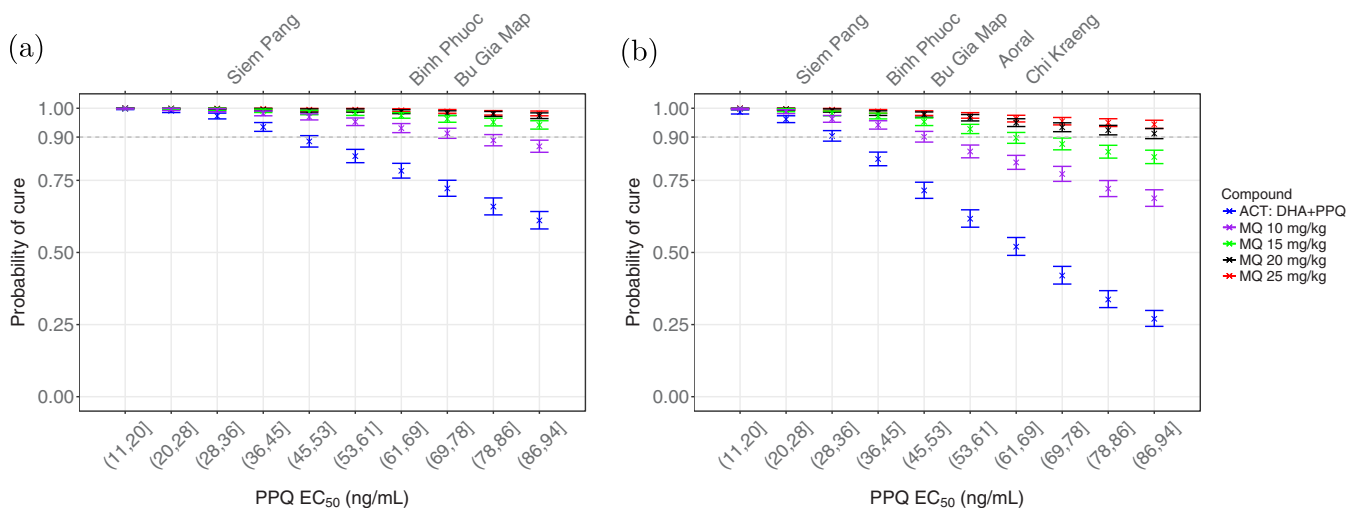


**FIG 3** The probability of cure on day 42 of follow-up when EC<sub>50</sub> of PPQ varies over the deciles of [11 94]. (a and b) Sensitivity (a) and resistance (b) to DHA. Blue, ACT treatment (the dosing regimens of PPQ and DHA are 18.0 mg/kg and 4.0 mg/kg, respectively, on days 1, 2 and 3); purple, a 10-mg/kg (3.3 mg/kg/day for 3 days) dose of MQ is added; green, a 15-mg/kg (5 mg/kg/day for 3 days) dose of MQ is added; black, a 20-mg/kg (6.7 mg/kg/day for 3 days) dose of MQ is added; red, a 25-mg/kg (8.3 mg/kg/day for 3 days) dose of MQ is added. The top labels show the geographical regions in South-East Asia (Table 1) where DHA-PPQ cure rates equal to the corresponding simulated values have been observed. Error bars show the 95% confidence intervals from Kaplan-Meier analysis.

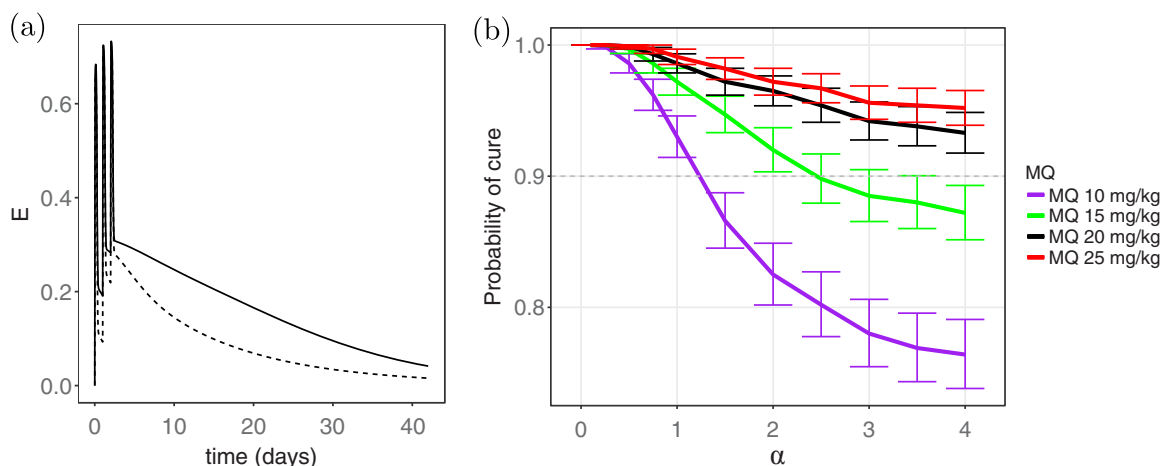


**FIG 4** Influence of antagonism between PPQ and MQ on the efficacy of the TACT. (a) Dashed and solid lines represent combined killing effect,  $E$ , for  $\alpha = 3.3$  and  $\alpha = 1$ , respectively. (b) Probability of cure on day 42 of follow-up versus the interaction parameter,  $\alpha$ , when the resistance level corresponding to Chi Kraeng is considered, i.e.,  $EC_{50} \in (69, 78]$ ; resistance to DHA is assumed. Different values of the interaction parameter,  $\alpha$ , produce synergism ( $0 < \alpha < 1$ ), zero interaction ( $\alpha = 1$ ), and antagonism ( $0 < \alpha < \infty$ ) in the combined effect of PPQ-MQ. The interpretation of the colors is explained in the caption to Fig. 3.

dose of MQ was needed to obtain a successful treatment in all of the regions. Of note, administering 25 mg/kg of MQ (8.3 mg/kg/day for 3 days), which is currently the recommended dosing regimen by the WHO for the ACT of MQ plus artesunate (19), can produce probability of cure above 90% at all of the DHA-PPQ resistance levels.

**Influence of the antagonistic PPQ-MQ interaction.** The effect of the PPQ-MQ interaction parameter,  $\alpha$ , on the probability of cure was then investigated. Figure 4a shows the combined killing effect of the drugs,  $E$ , over time for a selected patient with two different values of the interaction parameter:  $\alpha = 3.3$  (antagonism) and  $\alpha = 1$  (zero interaction); the other parameters were kept constant. The killing effect for  $\alpha = 1$  (solid line) is significantly higher than that for  $\alpha = 3.3$  (dashed line), indicating the extent to which the drugs can nullify each other's effect and the loss in the overall efficacy of TACT.

The effect of the interaction parameter,  $\alpha$ , on the efficacy was further assessed by restricting the resistance level to that corresponding to Chi Kraeng ( $EC_{50,P} \in (69,78]$ ), for instance, and estimating the probability of cure for different values of  $\alpha$ ; DHA resistance is also assumed. The results demonstrated a significant difference between the probabilities of cure at different values of  $\alpha$  (Fig. 4b), for example, when  $\alpha < 1$  (synergism), adding a 10-mg/kg dose of MQ was enough to provide 90% efficacy. In contrast, when  $\alpha > 1$  (antagonism), the probability of cure fell well below 90%. Similarly, the probability of cure declined with increasing  $\alpha$  (i.e., antagonism intensification) for MQ administration with higher doses. Of note, 20- and 25-mg/kg dosing regimens of MQ achieved greater than 90% efficacy at all values of  $\alpha$ , even at levels indicative of very strong antagonism. This highlights the robustness of these dosing regimens in producing a successful treatment. The antagonism between PPQ and MQ had an important impact on the efficacy of the TACT, and neglecting this may result in an underestimation of the dose of MQ required for successful treatment across different regions.

The effect of other manifestations of resistance on the efficacy of the TACT are illustrated in the supplemental material. Figure S1 presents the probability of survival at different levels of resistance produced by varying the maximum killing effect of PPQ,  $E_{max,P}$ . Similar to the case where  $EC_{50}$  was the manifestation of resistance, shown in Fig. 3, the results indicate that the three 6.7- or 8.3-mg/kg doses of MQ are sufficient to provide the desirable probability of cure at every level of resistance. The outcomes were consistent when the killing window of PPQ was shortened, as shown in Fig. S2 in the supplemental material. However, the probability of cure became extremely low, to an extent that the efficacy of 20-mg/kg dosing regimen fell below 90% at very high levels

of resistance, although observing such high resistance levels is currently unlikely. Nevertheless, a 25-mg/kg dosing regimen of MQ overcame such high levels of resistance and ensured high probability of cure.

## DISCUSSION

We have presented a novel mathematical model to investigate the efficacy of different regimens for triple artemisinin combination therapies (TACTs). Our analysis focused on DHA-PPQ-MQ, since DHA-PPQ is a widely used ACT in South-East Asia with declining efficacy in several locations (9–11). The addition of MQ to DHA-PPQ has potential to improve treatment, since the ACT of artesunate-MQ retains high efficacy, following its reintroduction as a first-line treatment in Cambodia (7). Our results suggest that a 10-mg/kg (3.3 mg/kg/day for 3 days) dose of MQ can improve the treatment efficacy of DHA-PPQ significantly and would be an appropriate regimen for regions such as Siem Pang in Cambodia and Binh Phuoc in Viet Nam. However, it is likely to be insufficient in regions where there is preexisting high-grade resistance to PPQ, such as Bu Gia Map in Viet Nam and Aoral and Chi Kraeng in Cambodia. Administration of DHA-PPQ with 15 mg/kg (3 mg/kg/day for 3 days) of MQ would be beneficial, but efficacy would still be compromised in the regions where there was high level of resistance to both PPQ and DHA, such as Chi Kraeng. To achieve a cure rate of greater than 90%, as recommended by the WHO, at least, 20 mg/kg (6.7 mg/kg/day for 3 days) of MQ needs to be administered in conjunction with the standard 3-day regimen of DHA-PPQ. As a result, the WHO-recommended dosing regimen of MQ, i.e., 25 mg/kg (8.3 mg/kg/day for 3 days), which has already been shown to be well tolerated and safe, has high potential to provide cure rates above 90%.

Our model enabled us to simulate the pharmacokinetics (PK) and pharmacodynamics (PD) following TACT administration to patients with malaria and provided important insights into the way in which the underlying mechanisms of drug action affect treatment efficacy. By taking account of between-patient and between-isolate variability, we were able to explore treatment efficacy across a wide range of different scenarios reflecting various parasite resistances to the different drug components. The results showed similar trends for different resistance manifestations, confirming the robustness of the proposed dosing regimen of DHA-PPQ-MQ.

We have proposed a novel empirical model to accommodate the effect of the combined drugs, assuming that PPQ and MQ (both quinoline compounds) have similar modes of action, which differs from that of DHA (an endoperoxide compound). The killing effects of PPQ-MQ and DHA were therefore assumed to be independent. This justified using a combination of Bliss independence and Loewe additivity to define the combined effect of the whole compound (see equation 1).

To facilitate the dissemination of our model and assist clinical researchers to investigate how different PK and PD parameters and dosing schemes influence parasitological outcomes, we produced an online application (appTACT [<http://lab.qmalaria.org/shiny/appTACT/>]) that allows varying the values of parameters and simulating the model.

Our mathematical model can be used to guide the development of suitable TACT regimens for investigation in clinical trials. Determining dosing regimens that are robust to a wide range of scenarios helps rationalize the logistical and financial challenges of phase 2 and 3 clinical trials. Further improvements in the model can be made to increase its fidelity to the underlying biology, for instance, by consideration of the artemisinins PK (e.g., bioavailability) dependence on parasite density (20) and different bioavailabilities of MQ at different administered days (21). The PD model can also be improved by incorporating more complexities underlying drug action, such as the dependence of killing effect on the timespan that parasites are exposed to drugs (22–25), immunity-mediated parasite killing (26, 27), and red blood cell (RBC) depletion/production (28, 29). However, in this initial analysis, we aimed to focus on the generality of the model and study worst-case scenarios, e.g., insignificant acquired immunity (patients living in low-endemicity regions), and negligible increased sensitivity of

**TABLE 2** Parameter values of the pharmacokinetic model<sup>a</sup>

| PK parameter        | Drug        |           |              | Description                   |
|---------------------|-------------|-----------|--------------|-------------------------------|
|                     | DHA (34)    | MQ (33)   | PPQ (35)     |                               |
| $k_a$ (1/h)         | 0.82 (26.5) | 0.29 (26) | 0.717 (168)  | Absorption rate               |
| CL/F (liters/kg/h)  | 1.01 (22.4) | 0.03 (33) | 1.38 (42)    | Clearance                     |
| V/F (liters/kg)     | 0.83 (50)   | 10.2 (51) |              | Vol of distribution           |
| $V_c/F$ (liters/kg) |             |           | 180.42 (101) | Vol of central compartment    |
| Q/F (liters/kg/h)   |             |           | 2.73 (85)    | Intercompartmental clearance  |
| $V_p/F$ (liters/kg) |             |           | 500 (50)     | Vol of peripheral compartment |

<sup>a</sup>The mean values are shown, along with the between-patient variabilities (presented as the percent coefficient of variation [%COV]) in parentheses.

parasites to MQ in some regions, associated with PPQ resistance (10, 30). Although we did not explore the degree to which the efficacy of TACT influenced other aspects of malaria control, such as the transmissibility of the parasite, this certainly warrants further investigation, since a more comprehensive perspective will be needed on the suitability of deploying TACT in areas of high drug resistance.

**MATERIALS AND METHODS**

**Mathematical Model.** The pharmacokinetic-pharmacodynamic (PK-PD) model presented in Zaloumis et al. (17) was used to model the dynamics of drug concentrations and parasite burden within an individual. In brief, this model describes the time-evolution of the number of parasites in the body,  $N$ , by the following difference equations:

$$N(a, t) = \begin{cases} N(a - 1, t - 1)(1 - E(a - 1, t - 1)), & 1 < a \leq 48, \\ N(48, t - 1)(1 - E(48, t - 1)) \times \text{PMF}, & a = 1, \end{cases}$$

where  $a$  is the parasites' age, taking only integer values over [1 48],  $t$  is time, and PMF is the parasite multiplication factor, which represents the number of merozoites released into blood by a shizont at the end of its life cycle.  $E(a, t)$  is the combined killing effect of the drugs and has been modified from that presented in Zaloumis et al. (17) to account for three drugs and accommodate drug interactions. The combined killing effect of the drugs is between 0 and 1 and is dependent upon the age of parasites during  $(t, t + 1)$ . The number of detectable parasites circulating in the blood,  $M(t)$ , is determined as follows:

$$M(t) = \sum_{a=1}^{48} N(a, t)g(a),$$

where  $g(a)$  accounts for the reduction in the number of circulating parasites in the blood due to sequestration, estimated to be:

$$g(a) = \begin{cases} 1, & a < 11, \\ 2^{\frac{11-a}{3}}, & a \geq 11, \end{cases}$$

where we assumed sequestration begins at age 11 and intensifies with age (16, 31). In the ensuing section, we explain the details of modeling the combined effect of the drugs,  $E$ .

Parasites can be cleared faster in patients who have acquired immunity to *P. falciparum*, although the effect is small relative to the effect of antimalarial drugs (32). Therefore, since a TACT regimen is sought that is as well effective in worst-case scenarios, e.g., in low-endemicity regions where resistance has been developed and acquired immunity within an individual is typically low, we did not incorporate the effect of immunity in the PD model. Red blood cell (RBC) depletion and production can also play important roles on the dynamics of malaria infection, as demonstrated earlier (28, 29). However, since the period between drug administration and the time to parasitemia recrudescence is of interest here, i.e., when RBC depletion is not yet significant, these factors are not incorporated in the model.

The PK models for the three drugs considered—DHA, PPQ, and MQ—are well characterized; one-compartment models were used for DHA and MQ, and a two-compartment model was used for PPQ (33–35). The PK parameter values are drawn from the literature and are provided in Table 2.

**Combined killing effect of the drugs.** The combined killing effect of the drugs is modulated by the manner in which they interact with each other. Synergistic interaction between drugs produces a stronger combined effect compared to the case where they do not interact, i.e., zero interaction (also known as pure additivity). Conversely, antagonistic drug-drug interactions can nullify their additive effect and produce a lower combined effect than that for the zero-interaction case. Therefore, to model the combined effect,  $E$ , we must first identify how the drugs interact.

An empirical approach was taken, modeling zero-interaction as the reference (null) model (36–38), since the mechanisms underlying the killing effects are complex and not completely understood (39). Among the existing empirical approaches of modeling zero-interaction, two are more prominent and

widely used: *Loewe additivity* (40) and *Bliss independence* (41). Loewe additivity is suggested to be a suitable concept for zero-interaction when noninteracting drugs have similar modes of action, however, when the drugs are believed to act independently, Bliss independence is more appropriate (37, 38).

It has been suggested that MQ and PPQ kill parasites through a similar mechanism, involving the disruption of heme detoxification in the parasite vacuole (39, 42, 43). DHA has a different mode of action, which involves the generation of free radicals and reactive intermediates that target various proteins of parasites (42, 44, 45). The PK and PD interactions of DHA with PPQ and MQ appear to be negligible (13).

The independent mechanisms of action of DHA and PPQ-MQ justifies using the Bliss independence concept for modeling the combined killing effect,  $E$ , given by

$$E = E_D + E_{PM} - E_D E_{PM}, \quad (1)$$

where  $E_D$  is the killing effect of DHA and  $E_{PM}$  is the combined effect of PPQ and MQ.

We assume Michaelis-Menten kinetics for  $E_D$ :

$$E_D = E_{\max,D} \frac{C_D^{\gamma_D}}{C_D^{\gamma_D} + EC_{50,D}^{\gamma_D}} \mathbf{1}_{W_D}(a),$$

where  $E_{\max,D}$  is the maximum killing effect of DHA,  $C_D$  is the DHA concentration,  $EC_{50,D}$  is the concentration at which 50% of the maximum killing effect is obtained,  $\gamma_D$  is the sigmoidicity (also known as slope) of the concentration-effect curve, and  $\mathbf{1}_{W_D}(a)$  is an indicator function, used to implement the age-specific killing of drugs, defined by:

$$\mathbf{1}_{W_D}(a) = \begin{cases} 1, & a \in W, \\ 0, & \text{otherwise,} \end{cases}$$

where  $W$  is the age window (interval) where the antimalarial drugs are able to kill the parasites and  $W_D$  is the killing window of DHA.

To define  $E_{PM}$ , models incorporating the Loewe additivity concept (as PPQ and MQ have similar modes of action) were used, which include only one parameter for the effect of the interaction between PPQ and MQ (37, 38, 46). These models are more specified to the framework of drug interaction, in contrast to the statistical models that usually have multiple parameters (47–49). A detailed description of the examined models is provided in Dataset S2 in the supplemental material. The final model selected was a combination of the models described by Talarida (38) and Machado and Robinson (46):

$$E_{PM} = E_{\max,P} \frac{C_{PM}^{\gamma_{PM}}}{C_{PM}^{\gamma_{PM}} + EC_{50,P}^{\gamma_{PM}}},$$

where

$$C_{PM} = \left( C_P^\alpha \mathbf{1}_{W_P}(a) + C_{eq,M}^\alpha \mathbf{1}_{W_M}(a) \right)^\frac{1}{\alpha}, \quad (2)$$

and

$$C_{eq,M} = E_P^{-1}(E_M(C_M)),$$

where  $E_M$  is the killing effect of MQ and  $E_P^{-1}$  is the inverse of the killing effect of PPQ, given by:

$$E_P^{-1}(x) = EC_{50,P} \left( \frac{x}{E_{\max,P} - x} \right)^\frac{1}{\gamma_P},$$

where  $E_{\max,P}$  and  $EC_{50,P}$  are the maximum killing effect of PPQ and the concentration at which half of the maximum killing effect is produced, respectively, and  $W_P$  and  $W_M$  are the killing windows of PPQ and MQ, respectively. Zero interaction is produced by equation 2 when  $\alpha = 1$ ; the values of  $1 < \alpha < \infty$  and  $0 < \alpha < 1$  produce antagonism and synergism, respectively. Note that PPQ is considered to be more potent than MQ (see Dataset S2 in the supplemental material for further information).

Isobolograms, widely used in pharmacology and toxicology studies, can inform on the nature of drug-drug interactions. These present data on the parasitocidal effect of paired drug concentrations. The combination of drug concentrations is then compared with the zero-interaction isobole (also known as linear isobole) (50) (see Fig. 5a). When the pairs of drugs concentrations are close to the linear isobole, zero-interaction is inferred, and when they lie significantly above or below the linear isobole, antagonism or synergism, respectively, can be inferred.

Using this approach, Davis et al. (13) showed that the paired PPQ and MQ data were significantly above the zero-interaction isobole (dashed line), indicating a strong antagonistic interaction between PPQ and MQ (Fig. 5a). The combined killing effect of PPQ-MQ,  $E_{PM}$ , was fitted to these data, and the PPQ-MQ interaction parameter was estimated to be  $\alpha = 3.3$ . Figure 5b shows the predicted  $E_{PM}$  for  $\alpha = 3.3$  for various PPQ and MQ concentrations. The killing effects of DHA and PPQ-MQ were applied to equation 1 to estimate the combined effect of DHA-PPQ-MQ and simulate the PD model (see Dataset S2 in the supplemental material for further details).

**Model simulation.** Latin Hypercube Sampling (LHS) was used to efficiently sample the parameter space (51) and simulate the PK profiles and parasitological responses. The distributions of the parameter values of the PK and PD models are presented in Tables 2 and 3, respectively. A triangular distribution was used for generating samples of  $\alpha$ , with a peak at  $\alpha = 3.3$ , estimated by fitting the model to the data, as explained in the previous section. The lower and upper bounds were selected to be 1 (zero interaction) and 10 (very strong antagonism), respectively. The initial parasite burden was assumed to have a log-normal distribution with a geometric mean of  $1.14 \times 10^{11}$  and a standard deviation of 1.13 on a log



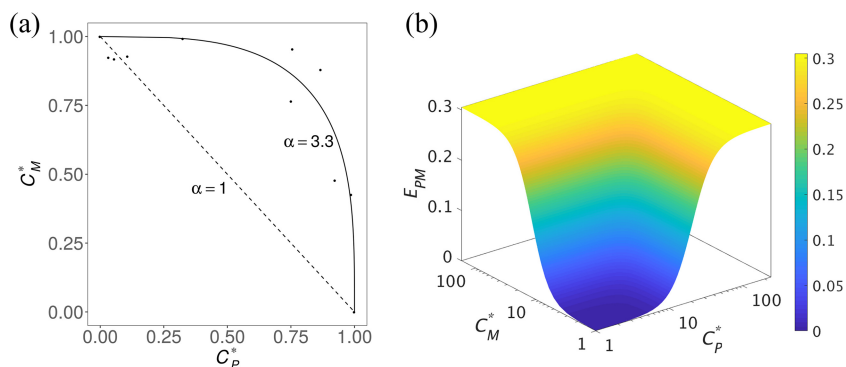


**FIG 5** Interaction between PPQ and MQ and their combined effect. (a) Isobologram presented in Davis et al. (13 [adapted with permission of the authors]) showing a strong antagonistic interaction between PPQ and MQ. The dashed and solid lines show the zero-interaction isobole and our fitted curve to the data points (estimated PPQ-MQ interaction parameter is  $\alpha = 3.3$ ), respectively.  $C_M^* = C_M/EC_{50,M}$  and  $C_P^* = C_P/EC_{50,P}$  are the normalized concentrations of MQ and PPQ, respectively. (b) Combined effect of PPQ and MQ, i.e.,  $E_{PM}$  (the  $C_M^*$  and  $C_P^*$  axes are log scaled), when PPQ-MQ interaction parameter ( $\alpha$ ) equals 3.3. The maximum killing effects and sigmoidicity of PPQ and MQ are considered equal (i.e.,  $E_{max,P} = E_{max,M} = 0.3$  and  $\gamma_P = \gamma_M = 3$ ) throughout the model fitting to conform with the data provided by Davis et al. 2006 (13).

scale. The corresponding 5th and 95th percentiles of parasitemia are  $1.78 \times 10^{10}$  and  $7.2 \times 10^{11}$ , respectively (Table 3).

The probability of cure (i.e.,  $1 -$  the probability of failure) was used as a measure of drug efficacy, and Kaplan-Meier survival analysis was carried out on simulated parasite versus time profiles of the patients to estimate the probabilities of cure at day 42 of follow-up. Treatment failure was defined as parasite recrudescence, in which the peripheral parasitemia exceeded the microscopic limit of detection (50 parasites/ $\mu$ l or a total parasite biomass of  $2.5 \times 10^8$ ).

Dosing regimens recommended by the WHO were used in the simulations. These included 18.0 mg/kg/day for PPQ and 4.0 mg/kg/day for DHA for 3 days. Current guidelines recommend a total dose of 25 mg/kg of MQ in combination with 4 mg/kg/day of artesunate (19). Splitting the dose of MQ (8.3 mg/kg/day for 3 days) improves the bioavailability of MQ, is better tolerated, and has a greater efficacy

**TABLE 3** Statistical distribution of the initial parasite burden and parameter values of the PD model<sup>a</sup>

| Parameter                      | Drug   | Distribution            | Description                                    |
|--------------------------------|--------|-------------------------|--|
| $N_0$                          |        | $\log N(25.46, 1.13)$   | Initial no. of parasites                       |
| $\mu_0$                        |        | $DU(4, 16)$             | Mean of initial parasites age distribution (h) |
| $\sigma_0$                     |        | $DU(2, 8)$              | SD of initial age distribution (h)             |
| PMF                            |        | $TRI(8, 12, 10)$        | Parasite multiplication factor (/48-h cycle)   |
| $E_{max}^b$                    | DHA    | $TRI(0.49, 0.69, 0.59)$ | Maximum killing effect                         |
|                                | PPQ    | $TRI(0.19, 0.50, 0.35)$ |  |
|                                | MQ     | $TRI(0.09, 0.43, 0.26)$ |  |
| $EC_{50}$ (ng/ml) <sup>c</sup> | DHA    | $U(1.44, 532.05)$       | Concn producing $E_{max}/2$ effect             |
|                                | PPQ    | $U(11.56, 94.19)$       |  |
|                                | MQ     | $U(20.48, 1087.22)$     |  |
| $\gamma$                       | DHA    | $\log N(1.31, 0.65)$    | Sigmoidicity of the concn-effect curves        |
|                                | PPQ    | $\log N(1.35, 0.66)$    |  |
|                                | MQ     | $\log N(0.97, 0.54)$    |  |
| $\alpha$                       | PPQ-MQ | $TRI(1, 10, 3.3)$       | Interaction parameter                          |

<sup>a</sup>Terms:  $TRI(l, h, m)$ , triangular distribution with peak at  $m$ , lower limit of  $l$ , and higher limit of  $h$ ;  $DU(l, h)$ , discrete uniform distribution with lower and higher limits  $l$  and  $h$ , respectively;  $U(l, h)$ , continuous uniform distribution with lower and higher limits  $l$  and  $h$ , respectively;  $\log N(\mu, \sigma)$ , log-normal distribution derived from a normal distribution with the mean  $\mu$  and standard deviation  $\sigma$ . The killing windows of the drugs were as follows (17):  $W_D = [6\ 44]$ ,  $W_P = [12\ 36]$ , and  $W_M = [18\ 40]$ .

<sup>b</sup>See Dataset S3 in the supplemental material for further details.

<sup>c</sup>The lower limit of the distribution of  $EC_{50}$  was chosen to be the *in vitro*  $IC_{50}$  (the concentration that inhibits the growth of parasites by 50%) of free drug, obtained by adjusting for the *in vitro* drug bindings. The higher limit was chosen to be half of the maximum drug concentration of the median of the PK profiles (17).

(52). Higher daily doses of MQ are associated with significant side effects (53), and thus modeling explored the minimum dosage of MQ that results in optimal efficacy. Hence, the administered dose of MQ was varied, and the corresponding TACT efficacy was estimated.

Different scenarios were considered, simulating resistance to DHA and/or PPQ. To simulate different degrees of PPQ and DHA resistance,  $EC_{50}$ ,  $E_{max}$ , and  $W$  were varied over the limited sampling intervals of the range of values given in Table 3. Since  $EC_{50}$  is not measurable in experiments, a wide initial range was considered for it: between the concentration that inhibits the growth of parasites by 50% *in vitro*,  $IC_{50}$  (adjusted for protein binding), and half the maximum concentration of the median of the PK profiles (17). As shown in Fig. 3, the limited sampling intervals for this range are able to produce the probabilities of cure observed in the regions with different levels of parasite susceptibility to drugs.

## SUPPLEMENTAL MATERIAL

Supplemental material for this article may be found at <https://doi.org/10.1128/AAC.01068-18>.

**SUPPLEMENTAL FILE 1**, PDF file, 0.2 MB.

## ACKNOWLEDGMENTS

This study was supported by the NHMRC Centres for Research Excellence in Malaria Elimination (1134989), Victorian Center for Biostatistics (1035261), Infectious Diseases Modeling to Inform Public Health Policy (1078068), an NHMRC Project Grant (1100394), and an ARC Discovery Project (DP170103076). F.J.I.F. was supported by Australian Research Council Future Fellowship. R.N.P. is a Wellcome Trust Senior Fellow in Clinical Science (200909), and J.A.S. is a NHMRC Senior Research Fellow (1104975).

## REFERENCES

- World Health Organization. 2017. World malaria report. World Health Organization, Geneva, Switzerland. <http://www.who.int/malaria/publications/world-malaria-report-2017/en/>.
- Fairhurst RM, Dondorp AM. 2016. Artemisinin-resistant *Plasmodium falciparum* malaria. *Microbiol Spectr* 4. <https://doi.org/10.1128/microbiolspec.E110-0013-2016>.
- Dondorp AM, Nosten F, Yi P, Das D, Phyo AP, Tarning J, Lwin KM, Arie F, Hanpithakpong W, Lee SJ, Ringwald P, Silamut K, Imwong M, Chotivanich K, Lim P, Herdman T, An SS, Yeung S, Singhasivanon P, Day NPJ, Lindegårdh N, Socheat D, White NJ. 2009. Artemisinin resistance in *Plasmodium falciparum* malaria. *N Engl J Med* 361:455–467. <https://doi.org/10.1056/NEJMoa0808859>.
- Ashley EA, Dhorda M, Fairhurst RM, Amaratunga C, Lim P, Suon S, Sreng S, Anderson JM, Mao S, Sam B, Sopha C, Chuor CM, Nguon C, Sovannaroeth S, Pukrittayakamee S, Jittamala P, Chotivanich K, Chutasmit K, Suchatsoonthorn C, Runchaoren R, Hien TT, Thuy-Nhien NT, Thanh NV, Phu NH, Htut Y, Han K-T, Aye KH, Mokuolu OA, Olaosebikan RR, Folarinmi OO, Mayxay M, Khanhavong M, Hongvanthong B, Newton PN, Onyamboko MA, Fanello CI, Tshefu AK, Mishra N, Valecha N, Phyo AP, Nosten F, Yi P, Tripura R, Borrmann S, Bashraheil M, Peshu J, Faiz MA, Ghose A, Hossain MA, Samad R, Rahman MR, Hasan MM, Islam A, Miotto O, Amato R, MacInnis B, Stalker J, Kwiatkowski DP, Bozdech Z, Jeeyapant A, Cheah PY, Sakulthaew T, Chalk J, Intharabut B, Silamut K, Lee SJ, Vihokhern B, Kunasol C, Imwong M, Tarning J, Taylor WJ, Yeung S, Woodrow CJ, Flegg JA, Das D, Smith J, Venkatesan M, Plowe CV, Stepniewska K, Guerin PJ, Dondorp AM, Day NP, White NJ. 2014. Spread of artemisinin resistance in *Plasmodium falciparum* malaria. *N Engl J Med* 371:411–423. <https://doi.org/10.1056/NEJMoa1314981>.
- Tun KM, Imwong M, Lwin KM, Win AA, Hlaing TM, Hlaing T, Lin K, Kyaw MP, Plewes K, Faiz MA, Dhorda M, Cheah PY, Pukrittayakamee S, Ashley EA, Anderson TJC, Nair S, McDew-White M, Flegg JA, Grist EPM, Guerin P, Maude RJ, Smithuis F, Dondorp AM, Day NPJ, Nosten F, White NJ, Woodrow CJ. 2015. Spread of artemisinin-resistant *Plasmodium falciparum* in Myanmar: a cross-sectional survey of the K13 molecular marker. *Lancet Infect Dis* 15:415–421. [https://doi.org/10.1016/S1473-3099\(15\)70032-0](https://doi.org/10.1016/S1473-3099(15)70032-0).
- Amato R, Lim P, Miotto O, Amaratunga C, Dek D, Pearson RD, Almagro-García J, Neal AT, Sreng S, Suon S, Drury E, Jyothi D, Stalker J, Kwiatkowski DP, Fairhurst RM. 2017. Genetic markers associated with dihydroartemisinin-piperazine failure in *Plasmodium falciparum* malaria in Cambodia: a genotype-phenotype association study. *Lancet Infect Dis* 17:164–173. [https://doi.org/10.1016/S1473-3099\(16\)30409-1](https://doi.org/10.1016/S1473-3099(16)30409-1).
- World Health Organization. 2017. Artemisinin and artemisinin-based combination therapy resistance. World Health Organization, Geneva, Switzerland. <http://www.who.int/malaria/publications/atoz/artemisinin-resistance-april2017/en/>.
- Simpson JA, Zaloumis S, DeLivera AM, Price RN, McCaw JM. 2014. Making the most of clinical data: reviewing the role of pharmacokinetic-pharmacodynamic models of anti-malarial drugs. *AAPS J* 16:962–974. <https://doi.org/10.1208/s12248-014-9647-y>.
- Amaratunga C, Lim P, Suon S, Sreng S, Mao S, Sopha C, Sam B, Dek D, Try V, Amato R, Blessborn D, Song L, Tullo GS, Fay MP, Anderson JM, Tarning J, Fairhurst RM. 2016. Dihydroartemisinin-piperazine resistance in *Plasmodium falciparum* malaria in Cambodia: a multisite prospective cohort study. *Lancet Infect Dis* 16:357–365. [https://doi.org/10.1016/S1473-3099\(15\)00487-9](https://doi.org/10.1016/S1473-3099(15)00487-9).
- Leang R, Taylor WRJ, Bouth DM, Song L, Tarning J, Char MC, Kim S, Witkowski B, Duru V, Domergue A, Khim N, Ringwald P, Menard D. 2015. Evidence of *Plasmodium falciparum* malaria multidrug resistance to artemisinin and piperazine in western Cambodia: dihydroartemisinin-piperazine open-label multicenter clinical assessment. *Antimicrob Agents Chemother* 59:4719–4726. <https://doi.org/10.1128/AAC.00835-15>.
- Phuc BQ, Rasmussen C, Duong TT, Dong LT, Loi MA, Ménard D, Tarning J, Bustos D, Ringwald P, Galappaththy GL, Thieu NQ. 2017. Treatment failure of dihydroartemisinin/piperazine for *Plasmodium falciparum* malaria, Vietnam. *Emerg Infect Dis* 23:715–717. <https://doi.org/10.3201/eid2304.161872>.
- Ariens EJ, Simonis AM. 1964. A molecular basis for drug action. *J Pharm Pharmacol* 16:137–157. <https://doi.org/10.1111/j.2042-7158.1964.tb07437.x>.
- Davis TME, Hamzah J, Ilett KF, Karunajeewa HA, Reeder JC, Batty KT, Hackett S, Barrett PHR. 2006. *In vitro* interactions between piperazine, dihydroartemisinin, and other conventional and novel antimalarial drugs. *Antimicrob Agents Chemother* 50:2883–2885. <https://doi.org/10.1128/AAC.00177-06>.
- Hodel EM, Kay K, Hastings IM. 2016. Incorporating stage-specific drug action into pharmacological modeling of antimalarial drug treatment. *Antimicrob Agents Chemother* 60:2747–2756. <https://doi.org/10.1128/AAC.01172-15>.
- Hoshen MB, Na-Bangchang K, Stein WD, Ginsburg H. 2000. Mathematical modelling of the chemotherapy of *Plasmodium falciparum* malaria with artesunate: postulation of “dormancy,” a partial cytostatic effect of the drug, and its implication for treatment regimens. *Parasitology* 121:237–246. <https://doi.org/10.1017/S0031182099006332>.
- Saralamba S, Pan-Ngum W, Maude RJ, Lee SJ, Tarning J, Lindegårdh N,

- Chotivanich K, Nosten F, Day NPJ, Socheat D, White NJ, Dondorp AM, White LJ. 2011. Intra-host modeling of artemisinin resistance in *Plasmodium falciparum*. Proc Natl Acad Sci U S A 108:397–402. <https://doi.org/10.1073/pnas.1006113108>.
17. Zaloumis S, Humberstone A, Charman SA, Price RN, Moehrle J, Gamobenito J, McCaw J, Jansen KM, Smith K, Simpson JA. 2012. Assessing the utility of an anti-malarial pharmacokinetic-pharmacodynamic model for aiding drug clinical development. Malar J 11:303. <https://doi.org/10.1186/1475-2875-11-303>.
  18. World Health Organization. 2018. WHO malaria threats map: tracking biological challenges to malaria control and elimination. World Health Organization, Geneva, Switzerland. <http://apps.who.int/malaria/maps/threats/>.
  19. World Health Organization. 2015. Guidelines for the treatment of malaria. World Health Organization, Geneva, Switzerland. <http://www.who.int/malaria/publications/atoz/9789241549127/en/>.
  20. Lohy Das J, Dondorp AM, Nosten F, Phyto AP, Hanpithakpong W, Ringwald P, Lim P, White NJ, Karlsson MO, Bergstrand M, Tarning J. 2017. Population pharmacokinetic and pharmacodynamic modeling of artemisinin resistance in Southeast Asia. AAPS J 19:1842–1854. <https://doi.org/10.1208/s12248-017-0141-1>.
  21. Price RN, Simpson JA, Teja-Isavatharm P, Than MM, Luxemburger C, Heppner DG, Chongsuphajaisiddhi T, Nosten F, White NJ. 1999. Pharmacokinetics of mefloquine combined with artesunate in children with acute falciparum malaria. Antimicrob Agents Chemother 43:341–346.
  22. Klonis N, Xie SC, McCaw JM, Crespo-Ortiz MP, Zaloumis SG, Simpson JA, Tilley L. 2013. Altered temporal response of malaria parasites determines differential sensitivity to artemisinin. Proc Natl Acad Sci U S A 110:5157–5162. <https://doi.org/10.1073/pnas.1217452110>.
  23. Dogovski C, Xie SC, Burgio G, Bridgford J, Mok S, McCaw JM, Chotivanich K, Kenny S, Gnädig N, Straimer J, Bozdech Z, Fidock DA, Simpson JA, Dondorp AM, Foote S, Klonis N, Tilley L. 2015. Targeting the cell stress response of *Plasmodium falciparum* to overcome artemisinin resistance. PLoS Biol 13:e1002132. <https://doi.org/10.1371/journal.pbio.1002132>.
  24. Cao P, Klonis N, Zaloumis S, Dogovski C, Xie SC, Saralamba S, White LJ, Fowkes FJL, Tilley L, Simpson JA, McCaw JM. 2017. A dynamic stress model explains the delayed drug effect in artemisinin treatment of *Plasmodium falciparum*. Antimicrob Agents Chemother 61:e00618-17. <https://doi.org/10.1128/AAC.00618-17>.
  25. Cao P, Klonis N, Zaloumis S, Khoury DS, Cromer D, Davenport MP, Tilley L, Simpson JA, McCaw JM. 2017. A mechanistic model quantifies artemisinin-induced parasite growth retardation in blood-stage *Plasmodium falciparum* infection. J Theor Biol 430:117–127. <https://doi.org/10.1016/j.jtbi.2017.07.017>.
  26. Winter K, Hastings IM. 2011. Development, evaluation, and application of an in silico model for antimalarial drug treatment and failure. Antimicrob Agents Chemother 55:3380–3392. <https://doi.org/10.1128/AAC.01712-10>.
  27. Challenger JD, Bruxvoort K, Ghani AC, Okell LC. 2017. Assessing the impact of imperfect adherence to artemether-lumefantrine on malaria treatment outcomes using within-host modeling. Nat Commun 8:1373. <https://doi.org/10.1038/s41467-017-01352-3>.
  28. Antia R, Yates A, de Roode JC. 2008. The dynamics of acute malaria infections. I. Effect of the parasite's red blood cell preference. Proc Biol Sci 275:1449–1458. <https://doi.org/10.1098/rspb.2008.0198>.
  29. McQueen PG, McKenzie FE. 2004. Age-structured red blood cell susceptibility and the dynamics of malaria infections. Proc Natl Acad Sci U S A 101:9161–9166. <https://doi.org/10.1073/pnas.0308256101>.
  30. Eastman RT, Dharia NV, Winzeler EA, Fidock DA. 2011. Piperaquine resistance is associated with a copy number variation on chromosome 5 in drug-pressured *Plasmodium falciparum* parasites. Antimicrob Agents Chemother 55:3908–3916. <https://doi.org/10.1128/AAC.01793-10>.
  31. Udomsangpetch R, Pipitaporn B, Silamut K, Pinches R, Kyes S, Looareesuwan S, Newbold C, White NJ. 2002. Febrile temperatures induce cytoadherence of ring-stage *Plasmodium falciparum*-infected erythrocytes. Proc Natl Acad Sci U S A 99:11825–11829. <https://doi.org/10.1073/pnas.172398999>.
  32. Ataide R, Ashley EA, Powell R, Chan J-A, Malloy MJ, O'Flaherty K, Takashima E, Langer C, Tsuboi T, Dondorp AM, Day NP, Dhorda M, Fairhurst RM, Lim P, Amarantunga C, Pukrittayakamee S, Hien TT, Htut Y, Mayxay M, Faiz MA, Beeson JG, Nosten F, Simpson JA, White NJ, Fowkes FJL. 2017. Host immunity to *Plasmodium falciparum* and the assessment of emerging artemisinin resistance in a multinational cohort. Proc Natl Acad Sci U S A 114:3515–3520. <https://doi.org/10.1073/pnas.1615875114>.
  33. Ashley EA, Stepniewska K, Lindegårdh N, McGready R, Hutagalung R, Hae R, Singhasivanon P, White NJ, Nosten F. 2006. Population pharmacokinetic assessment of a new regimen of mefloquine used in combination treatment of uncomplicated falciparum malaria. Antimicrob Agents Chemother 50:2281–2285. <https://doi.org/10.1128/AAC.00040-06>.
  34. Jansen KM, Duffull SB, Tarning J, Lindegårdh N, White NJ, Simpson JA. 2011. Optimal designs for population pharmacokinetic studies of oral artesunate in patients with uncomplicated falciparum malaria. Malar J 10:181. <https://doi.org/10.1186/1475-2875-10-181>.
  35. Tarning J, Ashley EA, Lindegårdh N, Stepniewska K, Phaiphun L, Day NPJ, McGready R, Ashton M, Nosten F, White NJ. 2008. Population pharmacokinetics of piperazine after two different treatment regimens with dihydroartemisinin-piperazine in patients with *Plasmodium falciparum* malaria in Thailand. Antimicrob Agents Chemother 52:1052–1061. <https://doi.org/10.1128/AAC.00955-07>.
  36. Chou T-C. 2006. Theoretical basis, experimental design, and computerized simulation of synergism and antagonism in drug combination studies. Pharmacol Rev 58:621–681. <https://doi.org/10.1124/pr.58.3.10>.
  37. Greco WR, Bravo G, Parsons JC. 1995. The search for synergy: a critical review from a response surface perspective. Pharmacol Rev 47:331–85.
  38. Tallarida RJ. 2006. An overview of drug combination analysis with isobolograms. J Pharmacol Exp Ther 319:1–7.
  39. Horn D, Duraisingh MT. 2014. Antiparasitic chemotherapy: From genomes to mechanisms. Annu Rev Pharmacol Toxicol 54:71–94. <https://doi.org/10.1146/annurev-pharmtox-011613-135915>.
  40. Loewe S. 1928. Die quantitativen probleme der pharmakologie. Ergebnisse Physiol 27:47–187. <https://doi.org/10.1007/BF02322290>.
  41. Bliss CI. 1939. The toxicity of poisons applied jointly. Ann Appl Biol 26:585–615. <https://doi.org/10.1111/j.1744-7348.1939.tb06990.x>.
  42. Combrinck JM, Mabothe TE, Ncokazi KK, Ambele MA, Taylor D, Smith PJ, Hoppe HC, Egan TJ. 2013. Insights into the role of heme in the mechanism of action of antimalarials. ACS Chem Biol 8:133–137. <https://doi.org/10.1021/cb300454t>.
  43. Davis TME, Hung T-Y, Sim I-K, Karunajeewa HA, Ilett KF. 2005. Piperazine Drugs 65:75–87.
  44. O'Neill PM, Barton VE, Ward SA. 2010. The molecular mechanism of action of artemisinin: the debate continues. Molecules 15:1705–1721. <https://doi.org/10.3390/molecules15031705>.
  45. Cravo P, Napolitano H, Culleton R. 2015. How genomics is contributing to the fight against artemisinin-resistant malaria parasites. Acta Trop 148:1–7. <https://doi.org/10.1016/j.actatropica.2015.04.007>.
  46. Machado SG, Robinson GA. 1994. A direct, general approach based on isobolograms for assessing the joint action of drugs in preclinical experiments. Stat Med 13:2289–2309. <https://doi.org/10.1002/sim.4780132202>.
  47. Carter WH, Gennings C, Staniswalis JG, Campbell ED, White KL. 1988. A statistical approach to the construction and analysis of isobolograms. J Am Coll Toxicol 7:963–973. <https://doi.org/10.3109/10915818809014527>.
  48. Gennings C. 2000. On testing for drug/chemical interactions: definitions and inference. J Biopharm Stat 10:457–467. <https://doi.org/10.1081/BIP-100101978>.
  49. Plummer JL, Short TG. 1990. Statistical modeling of the effects of drug combinations. J Pharmacol Methods 23:297–309. [https://doi.org/10.1016/0160-5402\(90\)90058-5](https://doi.org/10.1016/0160-5402(90)90058-5).
  50. Berenbaum MC. 1985. The expected effect of a combination of agents: the general solution. J Theor Biol 114:413–431. [https://doi.org/10.1016/S0022-5193\(85\)80176-4](https://doi.org/10.1016/S0022-5193(85)80176-4).
  51. McKay MD, Beckman RJ, Conover WJ. 1979. Comparison of three methods for selecting values of input variables in the analysis of output from a computer code. Technometrics 21:239–245. <https://doi.org/10.2307/1268522>.
  52. Simpson JA, Price R, Kuile F, Teja-Isavatharm P, Nosten F, Chongsuphajaisiddhi T, Looareesuwan S, Aarons L, White NJ. 1999. Population pharmacokinetics of mefloquine in patients with acute falciparum malaria. Clin Pharmacol Ther 66:472–484.
  53. Kuile FO ter, Nosten F, Luxemburger C, Kyle D, Teja-Isavatharm P, Phaiphun L, Price R, Chongsuphajaisiddhi T, White NJ. 1995. Mefloquine treatment of acute falciparum malaria: a prospective study of non-serious adverse effects in 3673 patients. Bull World Health Organ 73:631–642.